



LAWRENCE  
LIVERMORE  
NATIONAL  
LABORATORY

# PHOTONIC CRYSTAL AS A PASSIVELY DRIVEN STRUCTURE TO BOOST BEAM ENERGY

B. R. Poole, J. R. Harris, S. V. Milton

September 18, 2013

2013 Particle Accelerator Conference  
Pasadena, CA, United States  
September 29, 2013 through October 4, 2013

## **Disclaimer**

---

This document was prepared as an account of work sponsored by an agency of the United States government. Neither the United States government nor Lawrence Livermore National Security, LLC, nor any of their employees makes any warranty, expressed or implied, or assumes any legal liability or responsibility for the accuracy, completeness, or usefulness of any information, apparatus, product, or process disclosed, or represents that its use would not infringe privately owned rights. Reference herein to any specific commercial product, process, or service by trade name, trademark, manufacturer, or otherwise does not necessarily constitute or imply its endorsement, recommendation, or favoring by the United States government or Lawrence Livermore National Security, LLC. The views and opinions of authors expressed herein do not necessarily state or reflect those of the United States government or Lawrence Livermore National Security, LLC, and shall not be used for advertising or product endorsement purposes.

# PHOTONIC CRYSTAL AS A PASSIVELY DRIVEN STRUCTURE TO BOOST BEAM ENERGY\*

B.R. Poole<sup>#</sup>, LLNL, Livermore, CA 94550, USA

J.R. Harris, S.V. Milton, CO State University, Fort Collins, CO 80523, USA

## Abstract

The use of electromagnetic structures to couple energy to a charged particle beam is well known. These structures are usually driven by an external source of electromagnetic energy and the structure distributes that energy in such a way as being favorable to accelerate charged particles. Photonic crystals typically consist of periodic arrays of metal and/or dielectric structures spaced on a scale comparable to the wavelength of interest, have been investigated for use both as sources of microwave radiation and particle accelerators. In this case we consider driving a photonic crystal structure using a repetitive sequence of charge bunches driven from a photo-injector to resonantly excite the structure to produce an acceleration field to accelerate a suitably-delayed witness bunch to high energy. We examine the generation of the acceleration field as well as spurious modes. The dynamics of the witness bunch are examined to determine the longitudinal dynamics of the bunch and the energy spectra.

## INTRODUCTION

Periodic structures are commonly used in the accelerator community for particle accelerators and as slow wave structures for microwave sources. The use of an L-band RF source to drive an X-band linac structure consisting of a disk loaded waveguide to accelerate properly phased electron bunches has been described [1]. Periodic structures with alternative geometries may be considered for the same task. For example, a structure consisting of a waveguide with a periodic array of metal rings at two radii was demonstrated as a microwave source operating as a backward wave oscillator [2]. In this paper we consider several structures for use with an L-band source for passive acceleration including the disk loaded waveguide and two ring array geometries. The dispersion properties of various structures are determined using the COMSOL MultiPhysics RF package eigenmode solver [3]. The 2-D PIC code, OOPIC [4] is then used to examine the excitation of the X-band structure at the 9<sup>th</sup> harmonic of the 1.3 GHz L-band source. The effect of higher order modes (HOMs) are investigated as well as the dynamics of a witness bunch.

## MODELING AND SIMULATIONS

Three X-band structures were considered in this paper. All the structures were designed to have the same  $\pi$ -mode resonance at 11.7 GHz, the 9<sup>th</sup> harmonic of the 1.3 GHz

electron source by adjusting various geometric structure parameters. The only fixed parameter was the spatial periodicity  $d$ , to maintain the  $\pi$ -mode axial wavenumber  $k_z = \pi/d$ . The drive beam consisted of 6 MeV, 1.3 GHz Gaussian-like bunches with 100 A peak current, 10 ps FWHM, and 1.23 nC of charge per bunch with a bunch radius of 2 mm. The Fourier spectrum of the drive beam current is a comb of frequencies with 1.3 GHz spacing as shown in Fig. 1. The witness bunch is a single bunch injected into the linac after the cavity fields have been established, typically 50-100 ns into the simulation.

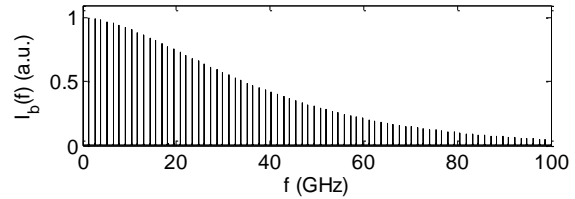


Figure 1: Beam current 1.3 GHz frequency comb.

## Disk Loaded Waveguide

The first structure considered is the disk loaded waveguide shown in Fig. 2

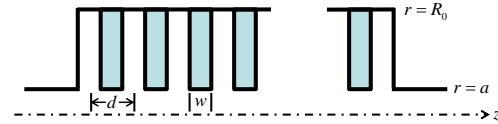


Figure 2: Disk loaded waveguide.

with  $R_0 = 1$  cm,  $a = 0.3$  cm,  $w = 0.2$  cm, and  $d = 1.2$  cm. The  $TM_{0n}$  dispersion properties are shown in Fig. 3 and Fig.4 shows the axial electric field distribution for the 11.7 GHz  $\pi$ -mode.

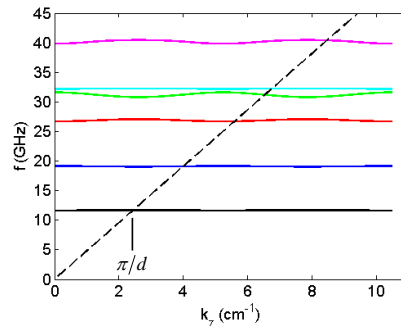


Figure 3:  $TM_{0n}$  modes of disk loaded waveguide.

The response of the structure to a single bunch was found using OOPIC to verify the various structure resonances. Figure 5 shows this response with resonances located at the intersection of the structure modes with the beam mode,  $\omega = k_z \beta c$ .

\* This work performed under the auspices of the U.S. Department of Energy by Lawrence Livermore National Laboratory under Contract DE-AC52-07NA27344  
#poole1@llnl.gov

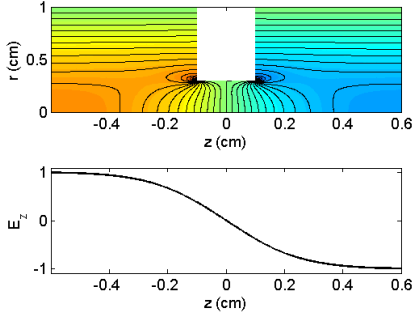


Figure 4: Axial electric field distribution at 11.7 GHz.

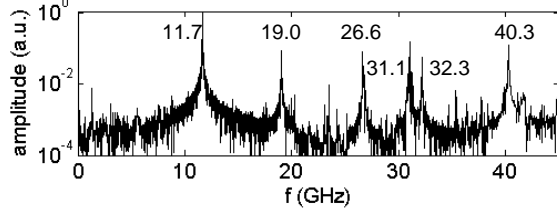


Figure 5: Single bunch response of disk loaded waveguide showing mode resonances.

A 1.3 GHz bunch sequence with the frequency comb spectra shown in Fig. 1 will resonantly excite the 9<sup>th</sup> harmonic 11.7 GHz  $\pi$ -mode in the linac structure. This field may then be used to accelerate a witness bunch to higher energy. Figure 6 shows a typical accelerating field greater than 1 MV/cm in the linac at 74.49 ns. The drive bunch has lost nearly 5 MeV of energy at this time.

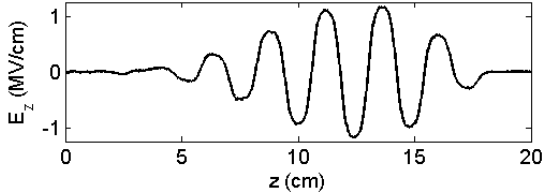


Figure 6: Acceleration field at 74.49 ns.

The evolution of the witness bunch energy distribution is shown in Fig. 7 and the evolution of the mean energy of both the drive and witness bunches shown in Fig. 8. The maximum acceleration gradient is 1.2 MV/cm producing an energy boost of nearly 7 MeV for the witness bunch.

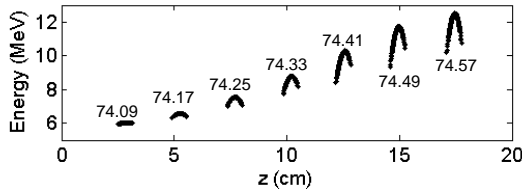


Figure 7: Snapshots of witness bunch energy distributions. The times indicated in the plot are in ns.

Note that the energy gain of the witness bunch benefits from the integrated energy stored in the linac structure accumulated from the previous drive bunches.

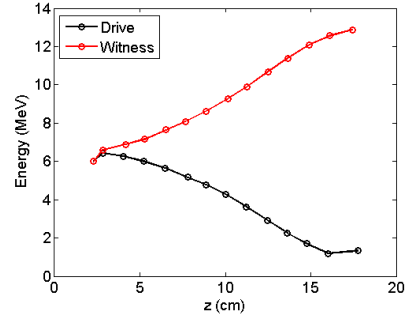


Figure 8: Mean energy of drive and witness bunches near the time of maximum acceleration gradient.

### Single Ring Array

The single ring array consists of an axial array of circular rings, in this case with rectangular cross-section as shown in Fig. 9.

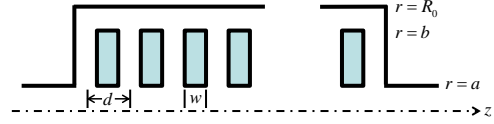


Figure 9: Single axial ring array loaded waveguide.

The structure dimensions are  $R_0 = 1.475$  cm,  $a = 0.3$  cm,  $b = 1.1$  cm,  $w = 0.2$  cm, and  $d = 1.2$  cm. Figure 10 shows the  $TM_{0n}$  dispersion properties.

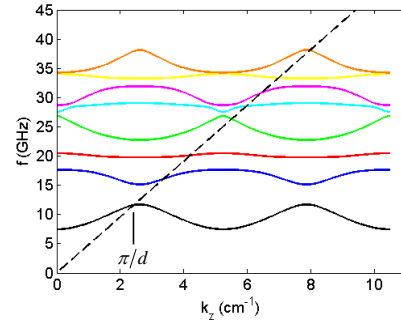


Figure 10:  $TM_{0n}$  modes of single ring array structure.

The dispersion curves in this structure exhibit much larger passbands compared to the disk loaded waveguide. There are also two additional modes for frequencies less than 40 GHz. This is due to increased coupling between the periodic cells and additional capacitance elements between the rings and the waveguide wall. Figure 11 shows the single bunch response for this structure which allows many additional discrete resonances in each of the modal passbands. It is easily seen in Fig. 11 that modes with larger passbands have more discrete resonances. The strength of these discrete resonances depends on the interaction with the bunch, the field distribution, as well as axial boundary conditions associated with the finite length periodic structure. Based on this spectral response, HOM's are expected to be more severe and tuning of the structure more difficult. Figure 12 shows the evolution of the drive and witness bunch mean energies showing an energy boost of only 4 MeV.

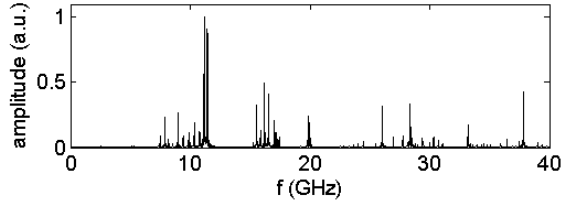


Figure 11: Single ring array single bunch response showing discrete resonances within each passband.

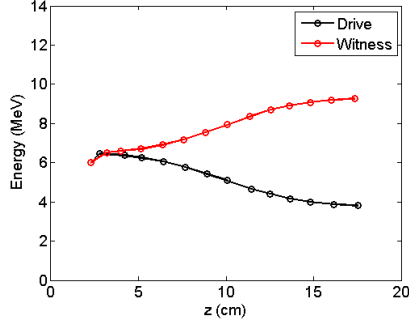


Figure 12: Mean energy of drive and witness bunches for single ring array structure.

### Double Ring Array

The double ring array consists of two radial layers of an axial array of circular rings as shown in Fig. 13

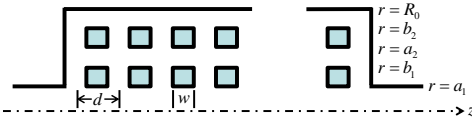


Figure 13: Double axial ring array loaded waveguide.

with  $R_0 = 1.73$  cm,  $a_1 = 0.3$  cm,  $b_1 = 0.7$  cm,  $a_2 = 1$  cm,  $b_2 = 1.4$  cm,  $w = 0.3$  cm, and  $d = 1.2$  cm. Figure 14 shows the  $TM_{0n}$  dispersion properties showing an additional mode for frequencies less than 30 GHz, and significantly wider passbands compared to the single array structure allowing for a significant number of discrete modes within each passband.

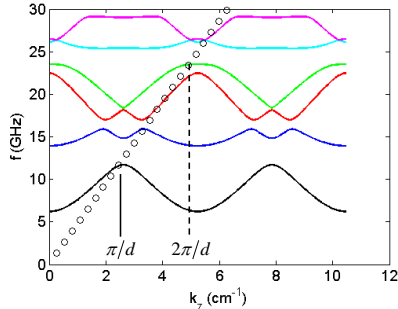


Figure 14:  $TM_{0n}$  modes of double ring array structure.

Also evident in Fig. 14 is the presence of a driven  $2\pi$ -mode resonance for the 4<sup>th</sup> mode near 23.4 GHz at the 18<sup>th</sup> harmonic of the L-band source. This mode is not an accelerating mode, and energy in this mode will not be available to accelerate the witness bunch. To detune the 23.4 GHz resonance, the outer ring layer was moved radially inward by 1 mm moving the resonance upward

by about 400 MHz. Simulations with the 1.3 GHz bunch sequence were run for the double ring array structure with both cases. Figure 15 shows a typical spectrum on axis for both cases. It is easily seen, that both resonances appear in the original structure (Case A) with the 23.4 GHz resonance dominating and after shifting the outer rings the 23.4 GHz resonance is eliminated and the 11.7 GHz resonance become prominent (Case B). Figure 16 shows the energy evolution for both cases showing an energy boost of 1 MeV for Case A and 1.8 MeV for Case B.

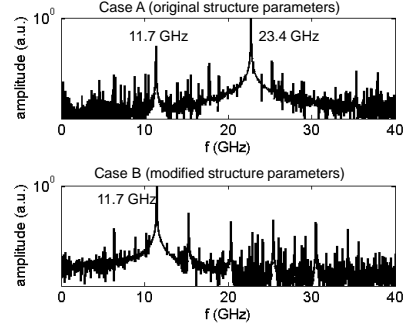


Figure 15: Double ring array response to 1.3 GHz bunch sequence showing effect of detuning 23.4 GHz mode.

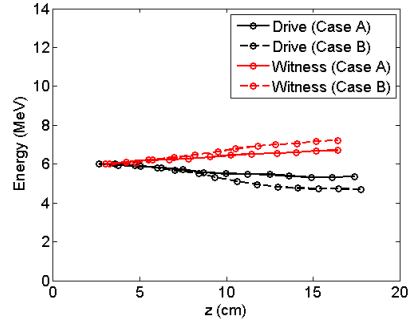


Figure 16: Mean energy of drive and witness bunches for double ring array structure.

## CONCLUSION

X-band linac structures for passive acceleration were studied for their effectiveness in providing an energy boost to a 6 MeV witness bunch when driven with a 1.3 GHz 6 MeV bunch sequence. It was found that the disk loaded waveguide was able to boost the energy by 7 MeV while the more open ring array structures provided more modest energy boosts. This was primarily due to the open nature of the ring structures and the presence of HOM's.

## REFERENCES

- [1] S. Biedron et al, "Passively Driving X-band Structures to Achieve Higher Beam Energies," IPAC'13, Shanghai, May 2013, TUPEA075, (2013); <http://www.JACoW.org>
- [2] D. Shiffler et al., IEEE Trans. On Plasma Sci. 38 (2010) 1462.
- [3] COMSOL MultiPhysics is a product of COMSOL, Inc. Burlington, MA; <http://www.comsol.com>
- [4] OOPIC is a product of Tech-X Corp., Boulder, CO; <http://www.txcorp.com>